DOI: 10.31276/VJSTE.65(1).81-88

Study on fabrication of ZnO@TiO_2 nanocomposite for perozone degradation of amoxicillin from aqueous solution

Thanh Diem Ngo Thi[1], Xuan Hoan Nguyen[1], Hiep Vu Phung[2], Minh Thanh Le[1], Lan Huong Nguyen[1*]

[1]Ho Chi Minh City University of Food Industry, 140 Le Trong Tan Street, Tay Thanh Ward, Tan Phu District, Ho Chi Minh City, Vietnam
[2]Southern Natural Resources and Environment Company, Ministry of Natural Resources and Environment, 30, No. 3 Street, Quarter 4, An Khanh Ward, Thu Duc City, Ho Chi Minh City, Vietnam

Received 14 October 2021; accepted 26 November 2021

Abstract:

In this study, a simple method for fabrication of a ZnO@TiO_2 nanocomposite was developed to degrade amoxicillin (AMX) from aqueous solution by heterogeneous photocatalytic perozone under UV irradiation (O_3/H_2O_2/ZnO@TiO_2/UV). ZnO nanoparticles were formed by the sol-gel method. The ZnO-NPs were then composited with commercial TiO_2 at modification ratios of 0, 10, 20, 30, 40, and 50% of ZnO-NPs to generate ZnO@TiO_2 nanocomposites. The physical-chemical characteristics of ZnO, TiO_2, and ZnO@TiO_2 at the optimal modification ratio were determined using S_{BET}, SEM, EDX, and XRD analysis. The catalytic activity of ZnO@TiO_2 was evaluated by degradation of AMX in an O_3/H_2O_2/ZnO@TiO_2/UV system. The results showed that 10%ZnO@TiO_2 exhibited the highest catalytic activity in degradation (in term of COD removal) of AMX with about 80% for 70 min of reaction time. This efficiency was higher than that of both systems using ZnO or TiO_2 only by double. This primary finding demonstrates the feasibility of 10%ZnO@TiO_2 photocatalysts in perozone systems to degrade persistent organic compounds in practical applications.

Keywords: **amoxicillin, ball milling, perozone, ZnO@TiO_2.**

Classification numbers: **3.4, 3.5**

1. Introduction

Nowadays, water source pollution by antibiotic residuals has become a global environmental problem. Owing to the difficult-to-degrade property of pharmaceutical residues, conventional methods can only partially treat these residues with high cost from industrial effluents [1-3]. As a result, there have been huge amounts of antibiotics discharged into receiving bodies leading to serious effects on human health and ecosystems, even at a low concentration [3, 4]. Among antibiotics, amoxicillin (AMX) is widely used to treat diseases and infections in almost all countries [5]. However, only 10-20% of amoxicillin is ingested by the human body and other organisms [5]. Indeed, AMX has been detected in almost every media such as surface water, domestic and industrial wastewater [6, 7], hospital waste [8], and secondary treated effluent with concentrations ranging from several ng/l to mg/l [9]. Thus, it is necessary to remove AMX residues from these media to conserve water resources for sustainable development.

Advanced oxidation processes (AOPs) are one of the most effective methods for the removal of antibiotic residuals because they possess several advantages such as high oxidation rate, no-secondary pollution, and non-selective oxidation of POPs through the continuous generation of hydroxyl radicals [2, 5, 10-12]. Among AOPs, ozonation- and photocatalysis-based AOPs have been proven effective at the removal of various persistent organic pharmaceutical contaminants [13-18]. However, using ozonation and photocatalysis processes separately meets some drawbacks such as high cost, low stability, low solubility in water, and slow oxidation rates. Thus, in order to overcome these disadvantages, ozonation has recently been combined with various heterogeneous photocatalysis processes to promote overall treatment efficiency [19, 20].

Titanium dioxide (TiO_2) and zinc oxide (ZnO) are photocatalysts that have been applied the most widely to photocatalytic oxidation processes [21, 22]. However, the application of TiO_2 alone in photocatalytic reactions has several limitations. The most conspicuous drawback of TiO_2 is its electron-hole recombination ability after excitation due to a high rate in recombination of photoinduced charge carriers [20-22]. This type of disadvantage leads

*Corresponding author: Email: huongnl@hufi.edu.vn

to difficulties in its practical application to wastewater treatment [13, 19]. Therefore, to overcome the disadvantages of TiO_2, a composite of TiO_2 with other semiconductors has been formed to improve its photolytic activity. In this study, ZnO nanoparticles were chosen to composite with TiO_2 thanks to its similarity in band gap energy (3.34 eV and 3.12 eV, respectively, for ZnO and TiO_2) [23]. Besides, ZnO also has photolytic catalytic activity and a reactive ability that is similar to TiO_2 under irradiation conditions. Especially, there are oxygen vacancies in ZnO NPs when they are fabricated using sol-gel. These oxygen vacancies in ZnO NPs indicate enhanced visible light activity for photocatalytic reactions [23]. The oxygen vacancy defects are also a main defect in TiO_2 materials, which could also play role as the photogenerated electron trapped sites. Thus, ZnO@TiO_2 can also be active under the visible light region [24-26]. For these reasons, ZnO is selected to couple with TiO_2 to form a composite photocatalyst that promotes synergistic effects of heterogeneous photocatalysis perozone to treat AMX in this study.

The aim of this study, therefore, is to develop ZnO@TiO_2 nanocomposites from ZnO nanoparticles and commercial TiO_2 with various modification ratios. Besides, the physical-chemical characteristics of the fabricated materials were described. Initial investigations about photocatalytic ability of obtained catalytic materials in degradation of AMX were also studied.

2. Materials and methods

2.1. Chemicals and materials

All chemicals with analytical grade, including commercial TiO_2, zinc acetate dihydrate ($Zn(CH_3COO)_2.2H_2O$, 99.9%), ethanol (C_2H_5OH, 99.0%), sodium hydroxide (NaOH, 99.9%), sulfuric acid (H_2SO_4, 98.0%), and hydrogen peroxide (H_2O_2, 30%) were purchased from Merck, Germany. Meanwhile, amoxicillin (AMX) was provided by Sigma Aldrich, Germany. Deionized water was used to prepare all chemical solutions.

2.2. Preparation of catalyst materials

In this study, the synthesis procedure of the TiO_2@ZnO composite nanomaterial consists of the following main steps. Firstly, TiO_2 and ZnO nanomaterials were separately synthesized by hydrothermal and sol-gel methods, respectively. For the synthesis of TiO_2 nanoparticles, a micrometre-sized commercial TiO_2 powder was mixed with 10 M NaOH solution and transferred into a sealed Teflon flask. The flask was then placed in an oven set to a constant temperature of 135°C and calcinated for 24 h. Afterward, the Teflon flask was cooled to room temperature (25±2°C), and the mixture in the Teflon flask was filtered and washed several times with hydrochloric acid and distilled water until a constant pH was reached. Finally, the obtained product was dried and calcinated at 300°C for 2 h to form TiO_2 nanoparticles. For the synthesis of ZnO nanoparticles, $Zn(CH_3COO)_2.2H_2O$ 99.9% was firstly mixed with citric acid at a molar ratio of 1:3. The mixture was then continuously magnetically stirred for 1 h at 80°C to achieve the sol-gel state. Next, this sol gel solution was kept at 135°C for 3 h to form xero-gel before calcination at 400°C for 5 h to form ZnO nanoparticles.

From the two synthesized TiO_2 and ZnO nanomaterials, the ZnO@TiO_2 composite nanomaterials were fabricated using ball milling for 2 h with varying ZnO contents of 10, 20, 30, 40 and 50% to form homogenous ZnO@TiO_2 nanocomposite. The synthesis process of ZnO@TiO_2 composite is illustrated in Fig. 1.

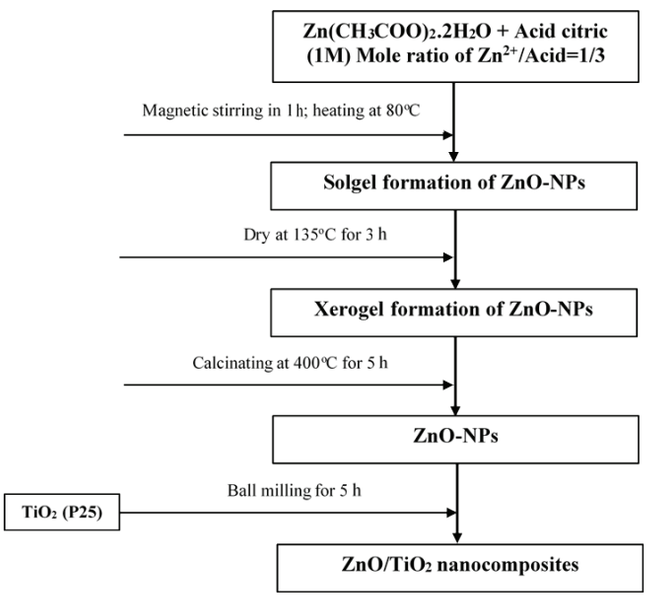

Fig. 1. Schematic description of the synthesis of ZnO@TiO_2 nanocomposites.

2.3. Experiment design

All experiments were performed on simulated wastewater samples with amoxicillin in the laboratory. The experimental set up of perozone degradation of amoxicillin is shown in Fig. 2. The experimental system is designed and installed to conduct research on the treatment of the antibiotic AMX with ozone using ZnO@TiO_2 at different composite ratios as photocatalysts.

AMX degradation was performed in batch experiments. Ozone was generated by an ozone generator (NextOzone 20P, Sinh Phu Joint Stock Company, Vietnam). The maximum capacity and input O_3 capacity at a flow of 15 ml/min were 5.0 g/h and 3.038 g/h, respectively. The oxygen source for the O_3 generator was taken from a pure oxygen tank. O_3 was continuously generated and distributed into a tubular borosilicate glass reactor with a height of 450 mm

and a diameter of 60 mm through a bubble air stone located at the bottom of the tank. The photocatalysts including ZnO, TiO_2 only, 10%ZnO@TiO_2, 20%ZnO@TiO_2, 30%ZnO@TiO_2, 40%ZnO@TiO_2, and 50%ZnO@TiO_2 were separately introduced into the reactors containing 500 ml of 100 mg/l AMX with a catalyst dose of 0.1 g/l at pH of 11 and H_2O_2 of 100 mg/l. Ozone aeration time was 10 min out of the 70 min of each cycle. The residual ozone in the outlet was absorbed by 1500 ml of 2% KI solution contained in a 2000-ml volumetric flask. The perozone reactions for AMX degradation were illuminated by two 35-W UV-Vis lamps at 320 nm. All heterogeneous catalytic perozone reactions were performed in parallel.

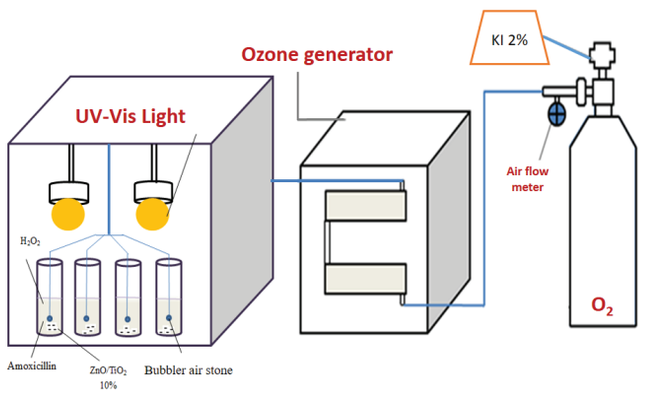

Fig. 2. Scheme of heterogeneous perozone degradation of AMX.

2.4. Analysis method

The N_2 adsorption-desorption isotherms at 77K were applied to analyse the textural properties of the catalysts including BET area, pore size, and pore diameter using Quantachrome Instruments version 11.0-NOVA. The morphology of the photocatalysts was observed by FESEM images using a Hitachi S-4800, Japan. The EDX data and mapping data were obtained by X-ray energy-dispersive spectroscopy analysis using a JSM-IT200 (InTouchScop). The phase composition and crystal structure of the nanomaterials before and after the catalytic process were determined by X-ray diffraction with a scanning speed of 1.25°/min at 2θ values between 20 and 80° using a Bruker D8 with Cu Kα emission (λ=0.1540 nm).

The degree of AMX degradation was assessed through COD measurement according to Standard Method 5220 [27]. pH was measured with a pH meter (Hach).

3. Results and discussion

3.1. Characteristics of catalysts

The effect of composite ratios between ZnO and TiO_2 on the textural properties of ZnO@TiO_2 was evaluated through nitrogen adsorption-desorption isotherms. The resulting data is indicated in Table 1. From this data, it can be seen that compositing ZnO with TiO_2 led to a slight decrease in the surface area and pore volume. Indeed, 10%ZnO@TiO_2 had an S_{BET} of 11.36 m^2/g, which is lower than that of TiO_2 and ZnO. This result was due to an aggregation of ZnO nanoparticles on the surface of TiO_2 [13]. The data in Table 1 also demonstrates that all photocatalysts are classified as a non-porous material because of their poor textural characteristics with low BET specific surface areas of 50.5, 20.6, and 11.36 m^2/g, total pore volume of 0.56, 0.089, and 0.044 cm^3/g and average pore diameters of 2.3, 0.102, and 0.123 nm, respectively, for ZnO, TiO_2, and 10%ZnO@TiO_2. The results suggest that the 10%ZnO@TiO_2 had no well-developed pore size to enhance its surface area. Thus, the contribution to the adsorption mechanism of AMX by 10%ZnO@TiO_2 was negligible in this study (data not shown).

Table 1. Nitrogen adsorption-desorption isotherm data of photocatalytic materials.

	Unit	ZnO	TiO_2	10%ZnO@TiO_2
S_{BET}	m^2/g	50.5	20.6	11.36
V_{pore}	cm^3/g	0.56	0.089	0.044
D_{pore}	nm	2.3	0.102	0.123

The morphological observation of 10%ZnO@TiO_2 through SEM data are presented in Fig. 3, which depicts 10%ZnO@TiO_2 before and after the perozone degradation of AMX. The surface morphology of 10%ZnO@TiO_2 was rough, heterogenous, and non-spherical with ZnO nanoparticles. The particles ranged from 100 to 200 nm in size and their shapes widely varied. Several pores have been narrowed due to surface aggregation of nanoparticles after the catalytic reaction.

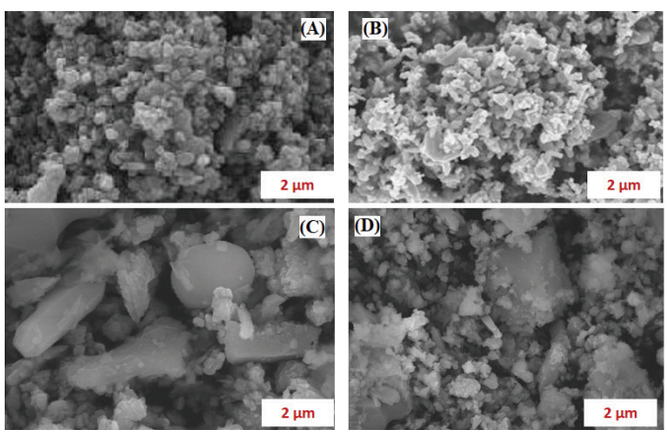

Fig. 3. SEM images of (A) TiO_2, (B) ZnO, and (C, D) 10%ZnO@TiO_2 before and after reaction, respectively.

The EDX spectrum of photocatalysts ZnO, TiO_2, and 10%ZnO@TiO_2 are shown in Fig. 4. The peak position indicates the existence of Zn and O on the EDX of ZnO

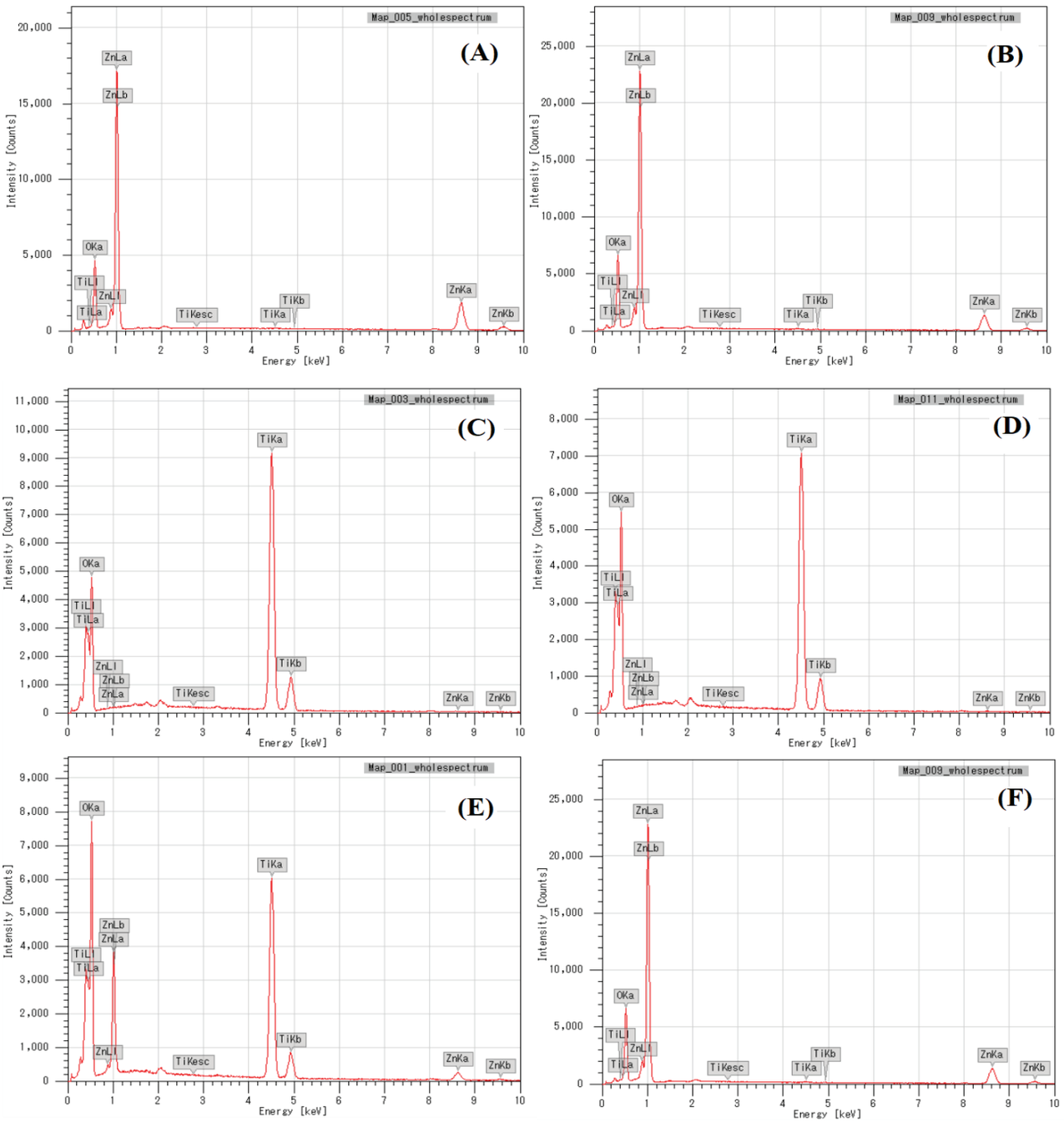

Fig. 4. EDX spectra of photocatalysts before and after reaction: (A, B) ZnO, (C, D) TiO_2, and (E, F) 10%ZnO@TiO_2.

nanoparticles and Ti and O on the EDX of TiO_2. There was an appearance of Zn atoms in the composite constituent of about 10% w.t. in 10%ZnO@TiO_2. The data in Fig. 4E confirmed again the presence of Zn, Ti, and O atoms in the sample. In addition, the EDX spectrum of photocatalysts ZnO, TiO_2, and 10%ZnO@TiO_2 showed that there was a negligible change in the content of Ti compared to Zn after the catalytic reaction (Fig. 4F). Similarly, the amount of Zn and Ti atoms in the ZnO and TiO_2 photocatalysts had an insignificant change, which affirmed the stability of the fabricated photocatalysts.

Figure 5 indicates the crystal structure of ZnO, TiO_2 and the 10%ZnO@TiO_2 composite before and after perozone degradation of AMX. The results are insignificantly changed after the photocatalytic process. As can be seen from the data in Fig. 5, in the XRD pattern of wurtzite ZnO, all the

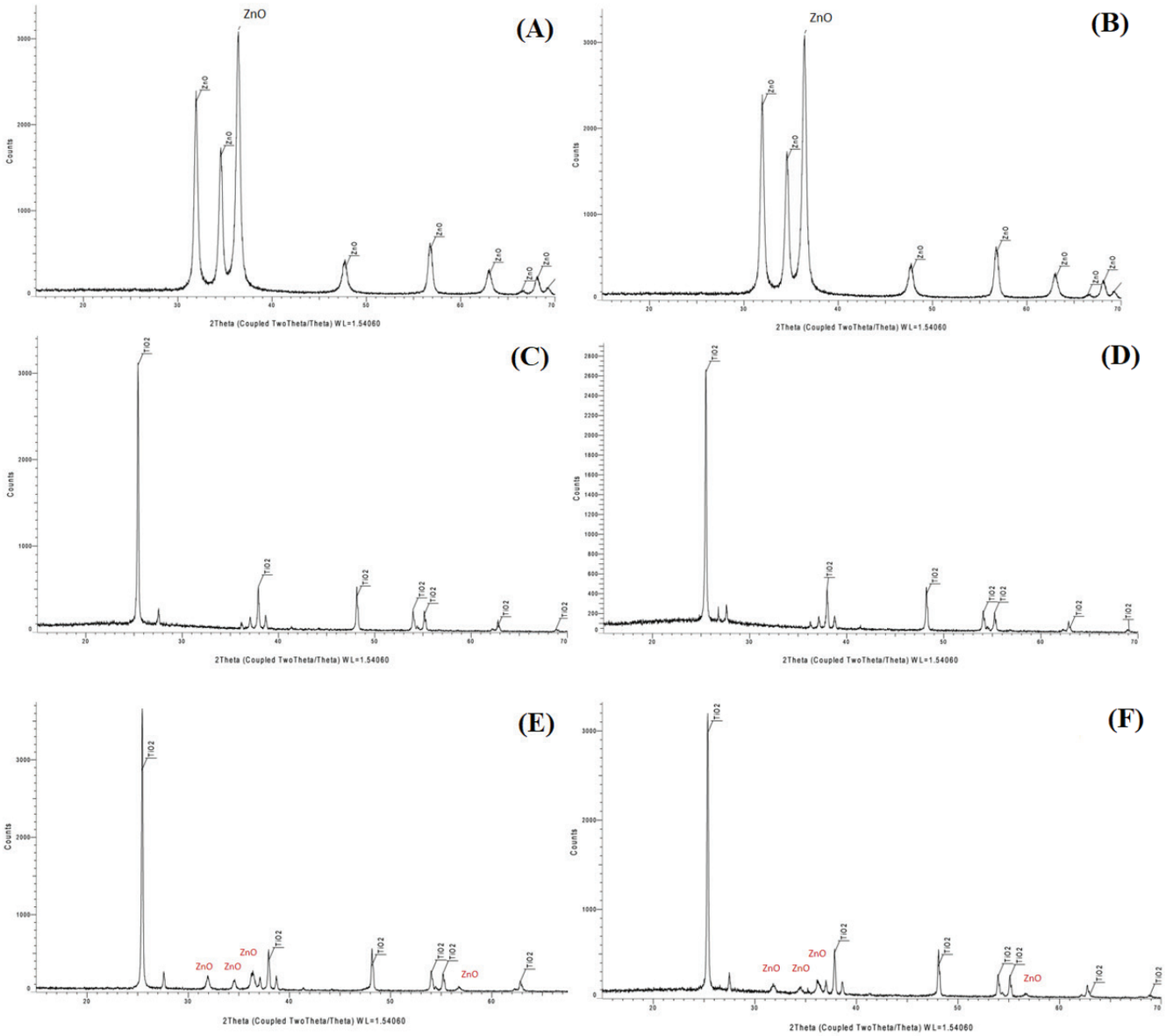

Fig. 5. XRD of the photocatalysts before and after reaction: (A, B) ZnO, (C, D) TiO_2, and (E, F) 10%ZnO@TiO_2.

typical peaks appeared at 2θ=31.94, 34.55, 36.42, 47.71, 56.8, 63.01, and 68.09º, corresponding to the (100), (002), (101), (102), (110), (103), and (112) planes of wurtzite ZnO, respectively (JCPDS card No. 36-1451). Besides, the peaks at 25.45, 37.92, 48.16, 53.97, 55.15, and 62.78º can be respectively ascribed to the (101), (004), (200), (105), (211), and (204) planes of the anatase phase of TiO_2 (JCPDS Card No. 21-1276). Similarly, the other peaks at 2θ = 27.54 and 36.16º correspond to (110) and (101) planes of the rutile phase of TiO_2 (JCPDS Card No. 21-1272) [28]. In the case of 10%ZnO@TiO_2, all typical diffraction peaks of both ZnO and TiO_2 appear in the XRD patterns of ZnO@TiO_2 composite [13]. This result elucidated the co-existence of both ZnO and TiO_2 in the nanocomposite. However, the peak intensity of ZnO is lower than TiO_2, which may explain the smaller content of ZnO compared with TiO_2 in the nanocomposite's composition.

3.2. Degradation of AMX by heterogeneous photocatalytic perozone

Effect of various modification ratios between ZnO-NPs and TiO_2 on AMX removal by heterogeneous photocatalytic perozone (O_3/H_2O_2/catalyst/UV) was carried out in batch reactors. The experiments were conducted at different ratios (w/w) of 10, 20, 30, 40, and 50% of ZnO-NPs with an initial AMX concentration of 100 mg/l, H_2O_2 concentration of 100 mg/l, and catalyst dosage of 0.1 g/l at pH 11 during 70 min of contact time. The obtained results are given in Fig. 6.

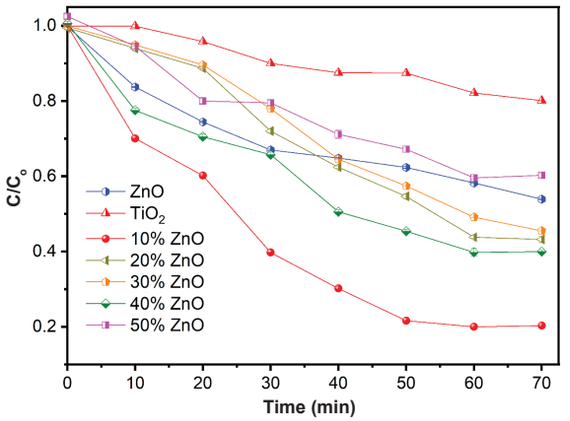

Fig. 6. Time dependence of AMX degradation by O_3/ZnO@TiO_2/H_2O_2/UV at various modification ratios between ZnO and TiO_2.

What stands out from the data in Fig. 6 is that there was a significant difference trend in AMX degradation between perozone systems. Specifically, the AMX perozone degradation by the system using only a TiO_2 catalyst was the lowest with 20.58%. The AMX removal efficiency achieved by O_3/H_2O_2/ZnO/UV was 41.12%, which was higher than that of O_3/H_2O_2/TiO_2/UV by double. However, when ZnO was composited with TiO_2, the AMX removal efficiency of perozone systems improved noticeably. Also, the AMX mineralization strongly depended on the composite ratio between ZnO and TiO_2. Specifically, the AMX removal reached a peak of 81.34% at a modification ratio of 10%, which was higher than that of O_3/H_2O_2/TiO_2/UV by four times and O_3/H_2O_2/ZnO/UV by double. Clearly, the ZnO@TiO_2 nanocomposite expressed excellent photocatalytic activity in comparison with TiO_2 particles and ZnO particles alone. However, when ZnO-NPs/TiO_2 composite ratios were further increased, the catalytic activity of the degradation of AMX by nanocomposite began a downward trend. The degradation of AMX was 62.85%, 59.67%, 60.87%, and 38.91%, respectively, at ZnO-NPs/TiO_2 ratios of 20, 30, 40, and 50% for 70 min of reaction time. An analogous result was reported by T. Yang, et al. (2018) [13] with an optimum modification ratio of 7% between ZnO and TiO_2 for salicylic acid (SA) removal by photocatalytic ozonation due to enriched surface hydroxyl groups of the modified catalyst. The degradation of SA decreased by 10% at a modification ratio of 10%. The degradation rate of ciprofloxacin by photocatalytic ozonation using a TiO_2/carbon dots catalyst dropped with an increase in doping ratio (k=0.320/min for 6 wt% TiO_2/CDs and k=0.247/min for 8 wt% TiO_2/CDs) [4]. In this study, an optimal result was obtained by loading 10% ZnO-NPs on TiO_2. This demonstrated that the combination of ZnO and TiO_2 has significantly enhanced the perozone degradation reaction under UV irradiation of pure TiO_2.

The mineralization kinetics of AMX in aqueous solution were investigated using heterogeneous catalytic perozone processes with photocatalysts at various modification ratios under the most suitable conditions determined by our previous study, which consisted of a pH of 11, catalyst dosage of 0.1 g/l, H_2O_2 concentration of 100 mg/l, and initial AMX of 100 mg/l. The general equation that describes the oxidation reaction of AMX can be written as follows:

$$AMX + {\cdot}OH \rightarrow nCO_2 + mH_2O + \text{intermediates} \quad (1)$$

The reaction rate in Eq. 1 can be described by following kinetic equation:

$$r = k.[C]^a.[OH^*]^b \quad (2)$$

where r is reaction rate (h^{-1}), k is reaction rate constant, and a and b are the reaction orders. However, the advanced oxidation reactions for the degradation of persistent organic compounds is mainly based on the continuous production of hydroxyl radicals with extremely short existence times. Thus, it can assumed that the amount of hydroxyl radicals would reach an equilibrium (i.e., [*OH] = constant). Then, Eq. 2 can be rewritten:

$$r = k'.[C]^a \quad (3)$$

Under the assumption that a perozone reaction follows both pseudo-first-order and pseudo-second-order kinetics, the integral of both sides of Eq. 3 (with a=1 for pseudo-first-order and a=2 for pseudo-second-order kinetics):

$$ln\frac{[C]_o}{[C]_t} = k'.t \quad (4)$$

$$\frac{1}{[C]_t} - \frac{1}{[C]_o} = k''.t \quad (5)$$

From the experimental data, the plot of and versus reaction time was made and the following correlation coefficients (R^2) were obtained: 0.9785 and 0.7678 for pseudo-first-order and pseudo-second-order kinetics, respectively. The obtained results showed that the data was fit to a straight line and the apparent first-order rate constant, k, corresponded to the slope of the straight line. Thus, in this study, the pseudo-first-order kinetic equation was applied to describe the effect of reaction conditions on heterogeneous photocatalytic perozone processes as in:

$$Ln\frac{C}{C_o} = -k_d.t \quad (6)$$

where, C_0 and C are the initial concentration of pollutant at the initial time and after t min of reaction, respectively, k_d is the degradation rate constant, and t is the degradation time.

By plotting ln C/C_o versus reaction time under optimum conditions, the calculated kinetic parameters for the degradation of AMX by heterogeneous photocatalytic perozone systems using the photocatalysts are demonstrated in Fig. 7.

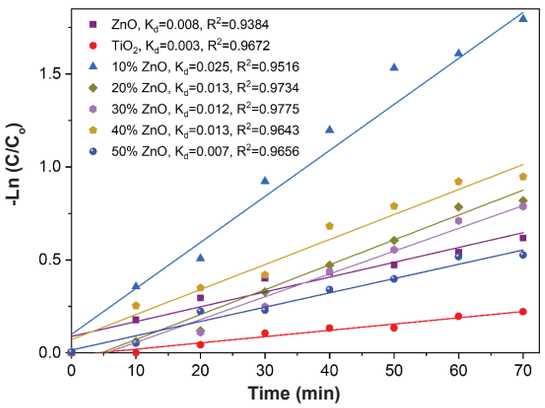

Fig. 7. Degradation kinetics of AMX by O_3/ZnO@TiO_2/H_2O_2/UV.

As expected, all computed k_d values had good agreement with the discussed results of mineralization of AMX at various modification ratios between ZnO and TiO_2. At various modification ratio values, it is clear from Fig. 7 that in all perozone systems for the degradation of AMX, the k_d values followed descending order as follows: O_3/H_2O_2/10%ZnO@TiO_2/UV>O_3/H_2O_2/ZnO/UV>O_3/H_2O_2/TiO_2/UV. The k_d values were the highest at a modification ratio of 10%ZnO@TiO_2/UV with 0.025/min. The results showed that in coupled heterogeneous photocatalytic ozonation process, the synergetic effect of perozone (O_3/H_2O_2) and photocatalysis (10%ZnO@TiO_2/UV) participating in the ozonation reaction proved to enhance the reaction rate, which led to an improvement of the overall treatment efficiency of the contaminants [4, 13, 19, 29]. Also, it is clearly there was a remarkable effect in composite ratio of ZnO-NPs on catalytic activity of materials in perozone degradation of AMX.

3.3. Mechanism of degradation perozone of AMX

In this work, from literature analysis and the discussion of the above results, it is apparent that the maximum AMX mineralization efficiency of 81.0% was obtained by perozone using 10%ZnO@TiO_2 under pH of 11, which proves the main mechanism of AMX degradation by photocatalytic perozone was through *OH radicals. The doping of ZnO-NPs and TiO_2 overcame the drawback of recombination of electron-hole pairs (h^+, e^-). Specifically, XRD data (Fig. 4), SEM, TEM, EDX and mapping data (Fig. 5) indicated the existence of ZnO NPs and TiO_2 mainly in the form of anatase in the nanocomposite catalyst. Furthemore, the S_{BET} of 10%ZnO@TiO_2 was 11.36 m^2/g, which confirms that ZnO@TiO_2 can act as both an adsorbent and catalyst. This nanocomposite catalyst enhanced the adsorbance of AMX on the ZnO@TiO_2's surface, decomposed O_3, and reacted with H_2O_2 in the O_3/H_2O_2/10%ZnO@TiO_2/UV system to increase the production of more *OH radicals. Apparently, composition of TiO_2 with ZnO rose the electron-hole separation thanks to ZnO@TiO_2 acting as electron trap, and modified the surface characteristics of the photocatalyst [13, 28, 30]. The production of more *OH was due to O_3's electrophilic property towards photogenerated electrons generated by photoexcitation of the ZnO@TiO_2 catalyst. In this work, the AMX degradation by O_3 can occur through two major routes, which consist of direct and indirect decomposition of ozone in solution and interfacial interaction reactions between the absorbed AMX on the catalyst's surface and the free radicals formed during photocatalytic perozone. These reactions for perozone degradation of AMX can be described by:

$$ZnO@TiO_2\text{-}e^-_{CB} + O_2 \rightarrow ZnO@TiO_2\text{-}{}^*O_2^- \quad (7)$$

$$2ZnO@TiO_2\text{-}e^-_{CB} + 2O_3 \rightarrow O_2 + 2\ ZnO@TiO_2\text{-}{}^*O_2^- \quad (8)$$

$$2ZnO@TiO_2\text{-}{}^*O_2^- + H_2O \rightarrow H_2O_2 + 2OH^- + O_2 \quad (9)$$

$$ZnO@TiO_2\text{-}\ e^-_{CB} + H_2O_2 \rightarrow {}^*OH + OH^- \quad (10)$$

$$ZnO@TiO_2\text{-AMX} + h^+_{VB}\ ({}^*OH \text{ or } {}^*O_2^-) \rightarrow CO_2 + H_2O + \text{intermediates} \quad (11)$$

In conclusion, the joint application of photocatalysis and perozone could give a much higher ·OH radical yield than the photocatalysis alone, which explains the synergistic effect between ozone and the role of the photocatalyst in inhibiting recombination of the photogenerated electrons and holes. Based on above results and discussion, it is clear that the composite of ZnO nanoparticles considerably enhanced the mineralization efficiency of AMX thanks to its multiple roles when modified with TiO_2. The functions of ZnO doped with TiO_2 include increasing electron transfer, electron storage, and enriching –OH groups on the photocatalyst's surface.

4. Conclusions

In this study, ZnO-NPs with various contents were composited with commercial TiO_2 to fabricate ZnO@TiO_2 composites that exhibited a high photocatalytic activity of heterogeneous perozone degradation of AMX. Data about the characteristics of synthesized composite materials showed benefits for catalytic reactions due to inhibiting the recombination of photogenerated electrons and holes, which led to the enhancement of *OH content in order to mineralize AMX. The degradation efficiency of AMX was shown to depend strongly on the modification ratio of ZnO. A modification ratio of 10%ZnO produced the highest removal efficiency of AMX with 81%. Also, data about the properties of the photocatalyst indicated a high stability after reaction suggesting its feasibility in practical application to remove persistent organic compounds from wastewater.

CRediT author statement

Thanh Diem Ngo Thi and Lan Huong Nguyen: Conceptualization, Methodology, Software; Lan Huong Nguyen, Hiep Vu Phung: Data curation, Writing- Original draft; Xuan Hoan Nguyen and Lan Huong Nguyen: Visualization, Investigation, Supervision; Hiep Vu Phung, Minh Thanh Le: Conducted experiments, Software, Validation; Lan Huong Nguyen: Writing- Reviewing and

Editing. All authors provided critical feedback and helped shape the research, analysis and manuscript.

ACKNOWLEDGEMENTS

The study was supported by The Youth Incubator for Science and Technology Program, managed by Youth Development Science and Technology Centre - Ho Chi Minh Communist Youth Union and Department of Science and Technology of Ho Chi Minh City, Vietnam under the contract number 23/2020/HD-KHCNT-VU.

COMPETING INTERESTS

The authors declare that there is no conflict of interest regarding the publication of this article.

REFERENCES

[1] E.M. Rodríguez, et al. (2013), "Mechanism considerations for photocatalytic oxidation, ozonation and photocatalytic ozonation of some pharmaceutical compounds in water", *J. Environ. Manage.*, **127**, pp.114-124.

[2] N.F.F. Moreira, et al. (2015), "Fast mineralization and detoxification of amoxicillin and diclofenac by photocatalytic ozonation and application to an urban wastewater", *Water Res.*, **87**, pp.87-96..

[3] S. Rodriguez-Mozaz, et al. (2015), "Occurrence of antibiotics and antibiotic resistance genes in hospital and urban wastewaters and their impact on the receiving river", *Water Res.*, **69**, pp.234-242.

[4] Y. Zeng, et al. (2019), "Study on heterogeneous photocatalytic ozonation degradation of ciprofloxacin by TiO_2/carbon dots: Kinetic, mechanism and pathway investigation", *Chemosphere*, **227**, pp.198-206.

[5] F.S. Souza, et al. (2018), "Comparison of different advanced oxidation processes for the removal of amoxicillin in aqueous solution", *Environ. Technol. (United Kingdom)*, **39(5)**, pp.549-557.

[6] E. Zuccato, et al. (2010), "Source, occurrence and fate of antibiotics in the Italian aquatic environment", *J. Hazard. Mater.*, **179(1-3)**, pp.1042-1048.

[7] E.S. Elmolla, M. Chaudhuri (2010), "Degradation of amoxicillin, ampicillin and cloxacillin antibiotics in aqueous solution by the UV/ZnO photocatalytic process", *J. Hazard. Mater.*, **173(1-3)**, pp.445-449..

[8] E.A. Serna-Galvis, et al. (2017), "Degradation of highly consumed fluoroquinolones, penicillins and cephalosporins in distilled water and simulated hospital wastewater by UV_{254} and UV_{254}/persulfate processes", *Water Res.*, **122**, pp.128-138.

[9] S. Al-Maadheed, et al. (2019), "Antibiotics in hospital effluent and domestic wastewater treatment plants in Doha, Qatar", *J. Water Process Eng.*, **28**, pp.60-68.

[10] N. Nasseh, et al. (2020), "Preparation of activated carbon@ZnO composite and its application as a novel catalyst in catalytic ozonation process for metronidazole degradation", *Adv. Powder Technol.*, **31(2)**, pp.875-885.

[11] J. Jeong, et al. (2009), "Degradation of tetracycline antibiotics: Mechanisms and kinetic studies for advanced oxidation/reduction processes", *Chemosphere*, **78(5)**, pp.533-540.

[12] L.M. Pastrana-Martínez, et al. (2012), "Degradation of diphenhydramine pharmaceutical in aqueous solutions by using two highly active TiO_2 photocatalysts: Operating parameters and photocatalytic mechanism", *Appl. Catal. B Environ.*, **113-114**, pp.221-227.

[13] T. Yang, et al. (2018), "Enhanced photocatalytic ozonation degradation of organic pollutants by ZnO modified TiO_2 nanocomposites", *Appl. Catal. B Environ.*, **221**, pp.223-234.

[14] R. Saravanan, et al. (2013), "Enhanced photocatalytic activity of ZnO/CuO nanocomposite for the degradation of textile dye on visible light illumination", *Mater. Sci. Eng. C.*, **33(1)**, pp.91-98.

[15] D. Dimitrakopoulou, et al. (2012), "Degradation, mineralization and antibiotic inactivation of amoxicillin by UV-A/TiO_2 photocatalysis", *J. Environ. Manage.*, **98**, pp.168-174.

[16] F. Biancullo, et al. (2019), "Heterogeneous photocatalysis using UVA-LEDs for the removal of antibiotics and antibiotic resistant bacteria from urban wastewater treatment plant effluents", *Chem. Eng. J.*, **367**, pp.304-313.

[17] W. Yao, et al. (2018), "Pilot-scale evaluation of micropollutant abatements by conventional ozonation, UV/O_3, and an electro-peroxone process", *Water Res.*, **138**, pp.106-117.

[18] E. Illés, et al. (2014), "Ketoprofen removal by O_3 and O_3/UV processes: Kinetics, transformation products and ecotoxicity", *Sci. Total Environ.*, **472**, pp.178-184.

[19] A.C. Mecha, M.N. Chollom (2020), "Photocatalytic ozonation of wastewater: A review", *Environ. Chem. Lett.*, **18**, pp.1491-1507.

[20] M. Mehrjouei, et al. (2015), "A review on photocatalytic ozonation used for the treatment of water and wastewater", *Chem. Eng. J.*, **263**, pp.209-219.

[21] W.S. Koe, et al. (2020), "An overview of photocatalytic degradation: Photocatalysts, mechanisms, and development of photocatalytic membrane", *Environ. Sci. Pollut. Res.*, **27**, pp.2522-2565.

[22] M.R.D. Khaki, et al. (2017), "Application of doped photocatalysts for organic pollutant degradation - A review", *J. Environ. Manage.*, **198**, pp.78-94.

[23] P.V. Viet, et al. (2021), Facile ball-milling synthesis of TiO_2 modified ZnO for efficient photocatalytic removal of atmospheric nitric oxide gas under solar light irradiation", *Chem. Phys. Lett.*, **775**, DOI: 10.1016/j.cplett.2021.138642.

[24] S.N. Nguyen, et al. (2019), "Investigation on photocatalytic removal of NO under visible light over Cr-Doped ZnO nanoparticles", *ACS Omega.*, **4**, pp.12853-12859.

[25] T.K. Truong, et al (2019), "Effect of Cr doping on visible-light-driven photocatalytic activity of ZnO nanoparticles", *J. Electron. Mater.*, **48**, pp.7378-7388.

[26] L.P.P. Ha, et al. (2021), "Visible-light-driven photocatalysis of anisotropic silver nanoparticles decorated on ZnO nanorods: Synthesis and characterizations", *J. Environ. Chem. Eng.*, **9**, DOI: 10.1016/j.jece.2021.105103.

[27] American Public Health Association (2012), *Standard Methods for the Examination of Water and Wastewater*, 541pp.

[28] R. Zha, et al. (2015), "Ultraviolet photocatalytic degradation of methyl orange by nanostructured TiO_2/ZnO heterojunctions", *J. Mater. Chem. A.*, **3**, pp.6565-6574.

[29] C.V. Rekhate, J.K. Srivastava (2020), "Recent advances in ozone-based advanced oxidation processes for treatment of wastewater - A review", *Chem. Eng. J. Adv.*, **3**, DOI: 10.1016/j.ceja.2020.100031.

[30] F.A. Akgül (2016), "Influence of Ti doping on ZnO nanocomposites: Synthesis and structural characterization", *Compos. Part B Eng.*, **91**, pp.589-594.